

# 1 Dual-matrix 3D culture system as a biomimetic model of epithelial tissues

2

3 Diana Bogorodskaya<sup>1,2,¶</sup>, Joshua S. McLane<sup>1,2,¶</sup>, and Lee A. Ligon<sup>1,2,\*</sup>

4 <sup>1</sup>Department of Biological Sciences, <sup>2</sup>Center for Biotechnology and Interdisciplinary Studies, Rensselaer  
5 Polytechnic Institute, Rensselaer Polytechnic Institute, Troy, NY, USA

6 \* Corresponding author

7 E-mail: [ligonl@rpi.edu](mailto:ligonl@rpi.edu) (LL)

8

9 ¶ These authors contributed equally to this work.

10

## 11 ABSTRACT

12 Recent years have seen an unprecedented rise in the use of 3D culture systems, both in fundamental research  
13 and in more translational settings such as drug testing and disease modeling. However, 3D cultures often  
14 remain underused by cell biology labs, both due to technical difficulties in system setup and inherent  
15 drawbacks of many of the common systems. Here we describe an easy to use, inexpensive and rapidly  
16 assembled 3D culture system, suitable for generation of both normal polarized epithelial cysts and in-situ  
17 tumor spheroids. This system allows for exploration of many questions of normal and cancer cell biology,  
18 including morphogenesis, epithelial polarization, cell motility, intra- and intercellular communication,  
19 invasion, metastasis, and tumor-stoma interaction. The 3D cultures are made up of a stiffness tunable, dual-  
20 matrix model that can incorporate co-culture of multiple cell types. The model allows for increased  
21 physiological relevance by mimicking the organization, ligand composition and stiffness present *in-vivo*.  
22 The setup allows for a wide spectrum of manipulation, including removing cells from the system for  
23 DNA/protein expression, transfection and high-resolution imaging of live or fixed cells.

24

## 25 INTRODUCTION

### 26 Overview of 3D culture

27 The first attempts at culturing cells in 3D were made in the early 1980s, in particular with the pioneering  
28 work of Mina Bissell and her lab (Bissell 1988). 3D cell culture techniques made incremental progress over  
29 the years and slowly gained popularity in the scientific community, with an explosion of interest in the mid-  
30 2010s. In recent years, the interest in utilizing 3D cell cultures and organoids as an intermediate platform  
31 for drug discovery and toxicity studies has skyrocketed, with multiple techniques developed to bring 3D  
32 culture in compatibility with high-throughput systems (Wrzesinski 2015, Nierode 2016). Over the years,  
33 multiple advantages of 3D culture systems were highlighted, including increased physiological relevance,  
34 ability to dissect the cellular and molecular biology of structures and niches unavailable in 2D cultures,  
35 such as epithelial tubes, breast tissue acini and the tumor microenvironment. Currently 3D cell cultures are  
36 used to study a broad range of questions, including differentiation, toxicology, tumor biology,  
37 morphogenesis and tissue architecture, as well as general cellular properties such as gene or protein  
38 expression and cell physiology (Ravi 2015). Multiple culture systems are currently available, ranging from  
39 gel-like matrices made from biological extracellular matrix (ECM) components (i.e. Matrigel®, Collagen  
40 I), synthetic hydrogel scaffolds (i.e. PEG, PLA) and scaffold-free techniques, such as hanging drop, low-  
41 adhesion aggregation or forced flotation (Edmondson, 2015)

42

43 The general premise of a 3D culture system is to place an individual cell or a cell aggregate into a 3D  
44 matrix, typically a gel or a synthetic scaffold, in which the cells are allowed to grow in all directions. The  
45 properties of the matrix are chosen to ensure a physiologically relevant model, with stiffness, ligand  
46 presence, and matrix composition typically taken into account. The starting cellular material can also be  
47 varied in its level of organization and complexity – from a single cell, which will be allowed to propagate  
48 in 3D, to a pre-formed clump of cells, to an organoid with distinct tissue architecture.

49

50 However, the widespread adoption of 3D culture systems has been slow due to the technical difficulties of  
51 setting up and maintaining the systems as well as the limited toolbox of manipulations and analyses that  
52 have been developed to study cells confined in scaffolds. On one side, complicated protocols, high costs of  
53 reagents, and long wait times between system setup and ready to use 3D cultures, deter researchers from  
54 using 3D setups. On the other side, the limitations of many models, such as high batch-to-batch variability,  
55 difficulties manipulating gene expression in 3D, and extracting DNA and protein from the scaffold-  
56 confined cells have also contributed to the slow spread of 3D culture use (Katt 2016)

57

58 Here we present a new model system with distinct advantages over previous models. First, it is designed to  
59 represent the physiological organization of epithelial tissues, with cell aggregates that are surrounded by a  
60 model of the basement membrane, which are then further embedded in a collagen-I hydrogel modeling the  
61 ECM of connective tissue. In addition, we have developed tools to change the stiffness of this hydrogel to  
62 mimic tissues with different mechanical properties. Furthermore, we have developed this model to  
63 maximize efficiency and time-to-experiment readiness, and to minimize cost and complexity. And finally,  
64 we have refined a set of tools to allow the researcher to manipulate and analyze cells within this 3D culture  
65 system, which should expand the utility of this setup. This system can be used to address a wide variety of  
66 experimental questions, but here we will use two examples from our work on epithelial morphogenesis and  
67 on the tumor microenvironment to illustrate the flexibility of the protocol.

68

### 69 **3D culture of polarized epithelial cells**

70 Apical-basal polarization is one of the key processes of normal epithelial organization, with defects in  
71 polarization often being a hallmark of malignancy (Overeem 2015). When grown in 2D culture, epithelial  
72 cells can only achieve partial polarization, although an intermediate 2D/3D culture model, in which the  
73 cells are grown on filter inserts, does allow for the growth of polarized cells (Drubin 1996). However,  
74 embedding epithelial cells in a gel matrix not only provides conditions for full polarization, but also allows  
75 for investigating the cellular and molecular mechanisms implicated in the development of polarized tissues  
76 and tissue regeneration (Pollack 1998, Zegers 2003). Madin-Darby Canine Kidney cells (MDCK) are the  
77 gold standard model of normal epithelial cells. They have been extensively used in 3D cultures to derive  
78 insights regarding mechanisms and signaling behind cell-adhesion and polarization (Capra 2017,  
79 Balasubramaniam 2017), as well as morphogenesis and tubule formation (O'Brien 2004, Dolat 2014,  
80 Gierke 2012, Boehlke 2013). Other types of cells have been used productively in 3D cultures as well,  
81 including primary salivary human stem/progenitor cells (hS/PCs) (Ozdemir 2016), MCF10A breast  
82 epithelial cells (Qu 2015), human lung epithelia aggregates (A549), and others (Ravi 2014). However, most  
83 of these 3D culture systems involved growing cells in either Matrigel®, collagen-I, or a non-biological  
84 hydrogel like alginate or PEG. Matrigel® is a good biochemical model of the basement membrane, but  
85 when used as a hydrogel, it loses the structural organization of the sheet-like basement membrane, and

86 collagen-I, while a good biochemical and structural model of the connective tissue ECM, necessitates that  
87 the epithelial cells secrete their own basement membrane, which can take a significant amount of time.

88

### 89 **3D culture of cancer cells**

90 A research area that has significantly benefitted from the development of 3D cell cultures is using cancer  
91 cells to model the tumor microenvironment and tumor-stroma interactions. Collagen-I hydrogels were one  
92 of the earliest 3D methods used to study the response of cancer cells to the extracellular matrix (ECM)  
93 (Richards et al., 1983). Many reports have been published examining the behavior of tumor cells in  
94 collagen-I or other, more specialized or defined, 3D matrices, but few if any of these models were  
95 representative of the organization of pre-metastatic tumors. Cells from a tumor *in situ* are exposed to a  
96 different ECM than metastatic cells; specifically, a tumor *in situ* is encapsulated within a basement  
97 membrane (BM), while a metastatic cell has left the tumor site and invaded into the connective tissue  
98 stroma. The basement membrane and the stroma are composed of different constituent components. BM is  
99 primarily made up of type IV collagen, laminin, and heparan-sulphate proteoglycans (Kalluri, 2003), while  
100 the stroma is largely made up of type I collagen and elastin (Culav et al., 1999). The physical characteristics  
101 of the two compartments differ as well; a solid tumor is typically much stiffer than the surrounding stroma  
102 (Paszek et al., 2005; Levental et al., 2009). Therefore, a biomimetic model of a tumor *in situ* should consider  
103 the composition and physical properties of both compartments and the organization of the two  
104 compartments relative to each other.

105

106

## 107 **MATERIALS**

### 108 **Reagents**

- 109 • Acetic acid (glacial; C<sub>2</sub>H<sub>4</sub>O<sub>2</sub>)
- 110 • Bovine serum albumin (BPA; product BP9703, Fisher Scientific)
- 111 • Collagenase (product 02195109, MP Biomedicals)
- 112 • Collagen-I (product 150026, MP Biomedicals)
- 113 • Dimethyl sulfoxide (DMSO; product D2650, Sigma-Aldrich)
- 114 • Distilled water (ddH<sub>2</sub>O)
- 115 • DMEM (product 10-013-CV, Corning)
- 116 • Ethylene glycol-bis(succinic acid N-hydroxysuccinimide ester) aka PEG-diNHS (product E3257,  
117 Sigma-Aldrich)
- 118 • Glassware (bottles with caps: 100 mL, 1 L)
- 119 • Goat serum (product G6767, Sigma-Aldrich)
- 120 • Growth factor reduced Matrigel® (product 354230, Corning)
- 121 • Magnetic stirrer and stir bar
- 122 • OPTI-MEM I (product 31985-070, Life Technologies)
- 123 • Paraformaldehyde solution (product 18814, Polysciences Inc)
- 124 • SlowFade® Diamond (ThermoFisher Scientific)
- 125 • Sodium azide (NaN<sub>3</sub>; product 190385000, Acros Organics)
- 126 • Sodium chloride (NaCl; product S5886, Sigma-Aldrich)
- 127 • Sodium phosphate dibasic (Na<sub>2</sub>HPO<sub>4</sub>; product S5136, Sigma-Aldrich)
- 128 • Sodium phosphate monobasic (NaH<sub>2</sub>PO<sub>4</sub>; product 71505, Sigma-Aldrich)

- 129 • Sodium pyruvate (product 11360070)
- 130 • Triton X-100 (product BP151, Fisher Scientific)
- 131 •  $\mu$ -Slide 8-well Glass Bottom chamber slide (product 80827, Ibidi)
- 132 • 1.5 mL disposable microcentrifuge tubes
- 133 • 4D-Nucleofector® X Kit (product V4XC-1032, Lonza)
- 134 • 10 cm cell culture dishes (product 172958, Thermo Scientific)
- 135 • 15 mL disposable conical tube with cap (product 352097, Becton Dickinson)
- 136 • 35 mm tissue culture dishes (product 10861-586, VWR)
- 137 • 35 mm glass bottom microwell dish (product PG5G-1.5014-C)
- 138 • 50 mL disposable conical tube with cap (product 82018-050, VWR)
- 139 • 60 mm tissue culture dishes (product 10062-890, VWR)
- 140 • 96-well round bottom ultra-low attachment microplates (product 7007, Corning)
- 141 • 100 mm tissue culture dishes (product 10861-594, VWR)

142

### 143 **Equipment**

- 144 • Class II microbiological safety cabinet
- 145 • CO<sub>2</sub> cell culture incubator
- 146 • Fluorescent and light microscope (model DMI4000 B, Leica Microsystems)
- 147 • Forceps
- 148 • Hemocytometer
- 149 • Nutating shaker (model 117, TCS Scientific)
- 150 • Kimwipes (product S-8115, Kimberly-Clark)
- 151 • Pipettes with non-sterile and sterile plastic tips (P2, P20, P200 and P1000)
- 152 • Rotational shaker (product 6780-FP, Corning)
- 153 • Sterile spatula
- 154 • 4D-Nucleofector (units AAF-1002B, AAF-1002X, Lonza)

155

## 156 **METHOD AND PROTOCOL**

157

### 158 **Cell culture**

159 MDCK cells (product ATCC CCL34, American Type Culture Collection, Manassas, VA) were cultured in  
160 DMEM high glucose (Corning) supplemented with 10% fetal bovine serum (VWR, Radnor, PA), 1%  
161 penicillin/streptomycin (Corning, Corning NY) at 37 °C, 5 % CO<sub>2</sub>. MDA-MB-231 human mammary  
162 epithelial tumor cells (ATCC HTB-26, American Type Culture Collection, Manassas, VA) were cultured  
163 in DMEM (Mediatech, Manassas, VA) supplemented with 5% fetal bovine serum (Atlanta Biologicals,  
164 Lawrenceville, GA), L-glutamine (Mediatech, Manassas, VA) and penicillin/streptomycin (Mediatech,  
165 Manassas, VA) under 5% CO<sub>2</sub>. For both cell lines, cells from passage 5 – 25 were used.

### 166 **Preparation of polarized epithelial spheroids**

167 An overview of the epithelial spheroid model production protocol is depicted in Figure 1. Briefly, MDCK  
168 cells are harvested through trypsinization and counted. Pipette 250,000 cells in 1 mL of fresh culture media  
169 into a 15 mL conical tube. Then add 500  $\mu$ L of 3 mg / mL growth factor-reduced Matrigel® diluted in  
170 OPTI-MEM I media to the cell solution. This results in a final concentration of 1 mg/mL Matrigel®, which

171 is below the concentration necessary for gelation. This allows the basement membrane extracellular matrix  
172 (ECM) components in Matrigel® to adsorb to the cell surface and jumpstart the formation of the basement  
173 membrane. The tube should then be placed on its side in the incubator with the cap partially open to allow  
174 air exchange, and incubated overnight. This will allow the cells to coalesce into small cell clumps. Most  
175 epithelial cells will preferentially adhere to one another rather than the non-tissue culture plastic of the tube.  
176 If the cells adhere to the tube, try tubes from different manufacturers.

177  
178 Cell aggregates can then be left to mature into spheroids in the Matrigel® suspension, or immediately  
179 incorporated into collagen-I hydrogels (Figure 1 B and C). For growth in suspension, the 1.5 mL of spheroid  
180 preparation can be transferred to a 35 mm dish containing 1 mL of warm culture media and incubated for  
181 2 days at 37 °C under 5 % CO<sub>2</sub>. The suspension can then be transferred to a 60 mm dish containing 3 mL  
182 of warm culture media and incubated for additional 2-3 days.

### 183 184 **Incorporation of polarized epithelial spheroids into hydrogels**

185 Collagen-I should be re-suspended in 0.02 N acetic acid at 3 mg / mL. This collagen stock solution can be  
186 aliquoted and stored at 4 C°. Combine the collagen solution with neutralizing solution (0.52 M Sodium  
187 Bicarbonate, 0.4 M HEPES and 0.08 N Sodium Hydroxide) and OPTI-MEM media at a ratio of 615 : 312  
188 : 77 (collagen-I : OPTI-MEM: neutralizing solution) and keep the mixture on ice. To prepare to embed the  
189 spheroids, first coat the bottom of the wells of an 8-chamber slide with 50 µL of collagen solution to provide  
190 a layer of collagen-I on the surface; incubate the slides for 45 min at 37 °C to allow gelation.

191  
192 Spheroids can be embedded into gels either after being grown to full polarity in the dilute Matrigel®  
193 solution or after the initial overnight incubation with Matrigel®. To embed the spheroids, transfer 1 mL of  
194 spheroid solution to a 15 mL conical tube, briefly spin it down and wash by gentle pipetting with 4 mL of  
195 cell culture media, briefly spin down again, and re-suspend in 400 µL of fresh cell culture media. As above,  
196 combine collagen-I stock solution (3 mg / mL in 0.02 N acetic acid) with neutralizing solution and spheroids  
197 in culture media in the ratio of 615 : 312 : 77. Pipette 50 µL of the collagen mixture containing cells onto  
198 the previously coated 8-chamber slide wells and gently spread it out into an even layer with the pipette tip;  
199 incubate for 45 min at 37 °C to allow gelation. Add 350 µL of fresh warm cell culture media to each well  
200 after the incubation and maintain the slides at 37 °C incubator with 5 % CO<sub>2</sub>. Change culture media every  
201 third day or as needed.

### 202 203 **Preparation of tumor spheroids**

204 An overview of the epithelial spheroid model production protocol is depicted in Figure 2. Spheroids are  
205 prepared as described previously (McLane and Ligon, 2016). Briefly, MDA-MB-231 cells are harvested,  
206 trypsinized and counted. Aliquot 50,000 cells in 50 µL of culture media into wells of ultra-low attachment  
207 round bottom 96-well plates. Incubate plates at 37 °C under 5 % CO<sub>2</sub> for 48 hours, which allows the cells  
208 coalesce into clumps. To further facilitate tumor spheroid formation, add 25 µL of growth factor-reduced  
209 Matrigel® (3 mg / mL in OPTI-MEM I) for a final concentration of 1 mg/mL, which is below the critical  
210 gelation concentration of Matrigel®. Incubate the coalesced masses for an additional 24 – 48 hours. After  
211 secondary incubation, cells will form tight tumor spheroids with a basement membrane mimetic external  
212 layer.

### 213 **Incorporation of tumor spheroids into hydrogels**



214 Hydrogels are prepared as above. Briefly, collagen-I stock solution is combined with neutralizing solution  
215 and cell suspension media at a ratio of 615 : 312 : 77. Alternately, poly (ethylene glycol)-di (succinic acid *N*-  
216 hydroxysuccinimide ester) (PEG-diNHS) dissolved in DMSO (100 mg / mL, product E3257, Sigma-  
217 Aldrich, molecular weight 456.36) can be added to the gel to increase the gel stiffness by crosslinking the  
218 collagen fibers. In our hands, a ratio of 615 : 308 : 77 : 4 for collagen-I : suspension media: neutralizing  
219 solution: PEG-diNHS / DMSO resulted in a fourfold increase in gel stiffness (from ~200 Pa to ~800 Pa)  
220 (McLane and Ligon, 2015). These gels can also be pre-populated by stromal cells, such as fibroblasts by  
221 adding fibroblasts into the collagen solution prior to gelation (McLane and Ligon, 2016).

222  
223 To make spheroid-containing hydrogels, transfer pre-formed spheroids in 2  $\mu$ L media droplets to 10 cm  
224 dishes (eight spheroids per dish). Add 100  $\mu$ L of collagen-I solution to each spheroid droplet, briefly mixing  
225 in the pipette tip and re-depositing in the dish. Incubate dishes for 45 min at 37 °C to allow gels to form,  
226 then add 10 mL culture media to the dish and release the hydrogels from the surface with a spatula. Culture  
227 all hydrogels on an orbital shaker to ensure they do not reattach to the culture vessel.

228  
229 **Transfection of spheroids with plasmid DNA**  
230 To transfect cells in spheroids, allow them to form to the desired stage in suspension (e.g. grow epithelial  
231 spheroids to full polarity for 5 days). Wash 1 mL of spheroids in suspension as described above. Spin  
232 spheroids down gently to pellet and aspirate the media, then add 100  $\mu$ L of SE Cell Line 4D-Nucleofector®  
233 X Kit and transfect with 4  $\mu$ g of plasmid of choice. Here we used GFP plasmid (Clontech, currently Takara  
234 Bio USA, Fremont, CA) diluted in MilliQ sterile-filtered water (Figure 1C). Transfect the cells using the  
235 4D-Nucleofector protocol CA-152. After transfection, transfer the spheroids to a 35-mm dish with 2 mL of  
236 fresh warm media and leave spheroids for four hours to recover post-transfection. To form spheroid-  
237 containing hydrogels, collect the spheroids, briefly spin down and re-suspend in 400  $\mu$ L of culture media.  
238 The spheroids then can be seeded in collagen gels as described above. A simplified illustration of 3D  
239 transfection workflow is shown in Figure 1C.

## 240 **Immunocytochemistry**

241 The cells in the hydrogels can be stained for protein markers using conventional primary and secondary  
242 antibodies. The spheroids in gels are fixed with 4% paraformaldehyde in PBS for 45 min at 37°C, then  
243 permeabilized with 0.25% Triton-X in dH<sub>2</sub>O for 45 min at room temperature, washed briefly with PBS +  
244 0.05% sodium azide (PBS-NaN<sub>3</sub>), and blocked for 2 hr at room temperature or overnight at 4°C in blocking  
245 solution (5% goat serum, 1% BSA, 0.05% NaN<sub>3</sub> in PBS). Spheroids can then be incubated with primary  
246 antibodies diluted in PBS + 0.05% sodium azide overnight at 4°C. For that purpose, gels and diluted  
247 antibodies are placed in 1.5 mL conical tubes on a nutating shaker. Primary antibody incubation is followed  
248 by three PBS-NaN<sub>3</sub> washes, 60 minutes each. Then, secondary antibodies and stains, such as DAPI or  
249 phalloidin diluted in PBS + 0.05% sodium azide are applied overnight at 4°C. The three 60 min washes  
250 with PBS-NaN<sub>3</sub> are repeated after the overnight incubation. Fixed hydrogels with spheroids can be stored  
251 in 1.5 mL conical tubes in PBS-NaN<sub>3</sub>.

252 In the example shown here (Figure 3) the primary, antibodies used were: alpha tubulin @ 1: 500 (product  
253 T9026, Sigma-Aldrich, St. Louis, MO; Collagen-IV, product GTX26311, GeneTex, Irvine, CA). Secondary  
254 antibodies were used @ 1:300 (Alexa Fluor, Jackson labs, Bar Harbor, ME) together with rhodamine

255 phalloidin for f-actin (product P1951, Sigma-Aldrich, St. Louis, MO) and DAPI (4',6-diamidino-2-  
256 phenylindole).

## 257 **Microscopy**

258 The spheroids in the gels can be imaged at high magnification using both DIC and fluorescent microscopy.  
259 To prepare fixed cells for a imaging, place a gel in a 35 mm glass-bottom dish (MatTek), remove excess  
260 PBS with a Kimwipe and apply a drop of SlowFade® Diamond antifade mountant, allowing the gel to  
261 incorporate the antifade reagent for approximately 1 minute, and then placing a glass coverslip on top to  
262 flatten the gel, optionally adding a 1 g precision weight on top to further flatten the gel.

263 In the example shown here (Figure 3), imaging was done on an inverted microscope (DMI 4000B Inverted  
264 Microscope, LEICA Microsystems) outfitted with an ORCA-ER digital camera (Hamamatsu Photonics)  
265 and a Yokogawa spinning disc confocal using Volocity imaging software (Improvision/PerkinElmer).

266

## 267 **Cell isolation for nucleic acid or protein extraction**

268 Protein and nucleic acid can be extracted from the cells grown in hydrogels for use in western blotting,  
269 PCR, and other application. To isolate cells, treat the gels with collagenase (product 02195109, MP  
270 Biomedicals) at 10 mg/mL until gels are digested (30 to 60 min). During digestion, place the tubes on a  
271 rotational shaker at 37 °C and monitor the tubes in five minute increments until the gels are completely  
272 digested. Centrifuge the digested gels at 300 xg for 5 minutes to pellet cells, and aspirate the digested  
273 collagen with a pipette. Wash the cell pellets twice with PBS by re-suspending cells in 1 mL PBS and re-  
274 pelleting cells with 300 xg spin. The cells can be then frozen, or used for nucleic acid or protein extraction  
275 using standard protocols.

276

## 277 **RESULTS AND DISCUSSION**

278 Here, we present a method to generate a model epithelial tissue, in which the organization, composition and  
279 physical properties of the ECM are physiologically appropriate, composition is controlled, and stiffness can  
280 be tuned (McLane and Ligon, 2016). This model system can be used to recapitulate normal epithelial  
281 organization, or an early *in situ* tumor. In both cases, the cells are encased in a basement membrane, initially  
282 nucleated by Matrigel®, and then are surrounded by a stiffness-controlled stromal matrix, composed of  
283 type I collagen, in which stromal cells such as fibroblasts can also be embedded. Other ECM components  
284 can be added in to the stromal mixture as well to increase the physiological accuracy.

285

## 286 **Formation of normal polarized epithelial spheroids**

287 The spheroids formed with the dual matrix method show early and robust polarization. As shown in Fig. 3,  
288 spheroids at day 1 are composed of multiple cells, distinctly visible with F-actin labeling (red). By day 3,  
289 the cells in spheroids have begun to assume the columnar morphology characteristic of polarized epithelial  
290 cells, and the spheroid has also begun to establish a hollow core. By day 6, the cells in the spheroids show  
291 distinct polarized morphology, and the hollow core is fully formed. In comparison, single cells seeded in a  
292 collagen-I gel form a mostly disorganized clump of cells by day 3, and do not show signs of polarization  
293 (columnar cell morphology, hollow core formation) by day 6. This side-by-side comparison clearly  
294 illustrates the increased speed of polarization and spheroid formation in the dual-matrix system as compared  
295 with a single matrix collagen-I system.

296

297

## 298 **Formation of tumor spheroids**

299 Tumor cell spheroids formed with the dual matrix method demonstrate behaviors characteristic of a tumor  
300 *in-situ*, such as matrix invasion, while spheroids formed of cells of non-metastatic lineage do not (McLane  
301 and Ligon, 2016). This normalized behavior from non-metastatic cells, the expected original hypothesis, is  
302 not what has been historically observed in single matrix culture models and is apparently mediated by the  
303 establishment of a basement membrane prior to hydrogel incorporation. This clearly illustrates the  
304 importance of the dual matrix system and the ability to mimic the *in-vivo* microenvironment in comparison  
305 to single matrix systems.

306  
307

## 308 **Comparison with other methods**

309 For over 30 years, Collagen-I hydrogels have been used to model the three-dimensional cellular  
310 environment. Numerous other 3D culture methods have been developed as well (Kimlin et al., 2013),  
311 including, but not limited to, cell culture upon or within natural protein hydrogels of Matrigel®, fibrin,  
312 hyaluronic acid (Masters et al., 2004), chitosan (Azab et al., 2006), and alginate (Barralet et al., 2005) as  
313 well as non-biological substrates or hydrogels including polyvinyl alcohol (Martens, 2000), poly-L-lactic  
314 acid (McLane et al., 2014a; Wang et al., 2009), and polyethylene glycol (Sawhney et al., 1993). Many of  
315 these hydrogel types have been combined and/or chemically modified to gain specific structural or  
316 mechanical characteristics, such as pore size, fibril size, alignment, stiffness (Chenite et al., 2001; Munoz-  
317 Pinto et al., 2012; Roeder et al., 2002; Wang et al., 2010; Deng et al., 2010; McKay et al., 2014; Wang and  
318 Stegemann, 2011; Liang et al., 2011), or to modulate ligand availability (Liu et al., 2010; Yoshida et al.,  
319 1997; Krause et al., 2008; Swamydas et al., 2010; Gandavarapu et al., 2014). The method described here  
320 utilizes several of these hydrogel strategies to recapitulate two distinct characteristics of the epithelial  
321 microenvironment – the dual matrix type and tissue organization of a normal epithelial tissue or a mammary  
322 tumor *in situ*, as well as the altered mechanical properties of the tumor-associated stroma.

323

324 The stiffness of a collagen-I hydrogel can be modulated by varying parameters such as pH, gelation  
325 temperature and collagen concentration (Li et al., 2009; Yang et al., 2009; Plant et al., 2009), as well as by  
326 the incorporation of other biotic or abiotic materials (Wang and Stegemann, 2010; Ulrich et al., 2010;  
327 Batorsky et al., 2005; Li et al., 2012; Ulrich et al., 2011; Song et al., 2010; Deng et al., 2010; Krause et al.,  
328 2008). However, altering these parameters or incorporating a secondary material alters the structure of the  
329 hydrogel and/or availability of the collagen-I ligand. To avoid these potential changes, we control collagen-  
330 I hydrogel stiffness independently of pH, temperature and protein concentration and without the  
331 incorporation of a second material by crosslinking the collagen-I with poly-(ethylene glycol)-di (succinic  
332 acid N-hydroxysuccinimide ester) (PEG-diNHS) (Abdella et al., 1979). PEG-diNHS makes short crosslinks  
333 between proteins by forming amide bonds between the collagen-I and itself to tether collagen molecules  
334 together, which mimics cross-links formed *in vivo* (Wallace, 2003). These collagen-I PEG-diNHS  
335 hydrogels have been previously used in studies of tumor spheroid formation and in tissue engineering, and  
336 show good biocompatibility (Jeong et al., 2013; McLane and Ligon, 2015a; Liang et al., 2011). These  
337 hydrogels also have defined, reproducible matrix stiffness within the range of epithelial and mammary  
338 physiology (Levental et al., 2009; Paszek et al., 2005), in contrast to many studies of cell-matrix interaction  
339 which either greatly exceed the physiological range (Leight et al., 2012; Tilghman et al., 2010; Pathak and  
340 Kumar, 2012; Chia et al., 2012), or do not measure or consider the stiffness of their model system.

341



342 The basement membrane (BM) extracellular matrix is made up of different proteins from that of connective  
343 tissue, and those that are shared between the two are present in different concentrations (Shoulders and  
344 Raines, 2009). In the case of normal epithelial tissue or a carcinoma *in situ*, an early stage in tumor  
345 development in which the BM is still intact, the cells are surrounded by the BM. Tumor cells must degrade  
346 this BM or otherwise circumvent it before invading into the stromal tissue. Our model of both normal  
347 epithelial spheroids and of a tumor *in situ* utilizes Matrigel®, a commercially available sarcoma produced  
348 protein mixture rich in basement membrane proteins (Hughes et al., 2010), to jumpstart BM formation. To  
349 accomplish this, we form cell aggregates or spheroids in the presence of dilute Matrigel®. We use  
350 Matrigel® at a concentration below the critical gelation concentration, so it does not form a gel, but allows  
351 basement membrane components to be adsorbed to the surface of the cells during aggregate or spheroid  
352 formation. Most epithelial cells will also secrete basement membrane proteins and form a basement  
353 membrane by themselves, but this process can take over a week. By providing building blocks, we can  
354 significantly accelerate basement membrane formation. We then incorporate the BM-coated spheroid into  
355 a stromal mimetic collagen-I hydrogel. This creates an *in vivo*-like organization and matrix composition in  
356 which epithelial cells are encased in a BM surrounded by a stromal matrix and stromal cells. The  
357 organization of the model allows for the transmission of both chemical and mechanical signals between  
358 epithelial cells and the stromal matrix and any stromal cells incorporated in it. There are few other  
359 experimental systems currently in use which embed basement membrane coated spheroids into collagen-I  
360 stromal matrices of defined stiffness, although there are co-culture systems which allow for chemical  
361 signaling between cell types (Peng et al., 2013; Bischel et al., 2015) or which investigate cell-cell or cell-  
362 matrix interactions with multiple matrices, although the organization of the matrices may not be as  
363 physiologically relevant as ours (Viney et al., 2009; Krause et al., 2008; Swamydas et al., 2010).

364  
365 The most common 3D hydrogel based approach to investigate tumor cell invasiveness involves starting  
366 with a single cell suspension in a hydrogel and then allowing the cells to proliferate to form acinar structures  
367 (Chambers et al., 2011; Krause et al., 2008; Swamydas et al., 2010; Liang et al., 2011). Our model departs  
368 from this method by first forming epithelial tumor spheroids in the presence of basement membrane  
369 components to accelerate the formation of a basement membrane. These formed spheroids are then  
370 incorporated into the stromal matrix after a coherent structure in which the cells have developed significant  
371 apical-basal polarity has formed. We believe this is more representative of a tumor *in situ* and will yield  
372 more translational results as tumors develop from existing tissue, not from single cells within a matrix. We  
373 have recently used this method to show that spheroids of both normal MCF10A cells and more metastatic  
374 MDA-MB-231 cells behave somewhat differently than when grown in a less physiologically relevant  
375 system (McLane and Ligon, 2016). For example, it has previously been suggested that the phenotypically  
376 normal MCF10As become invasive when grown in a stiff matrix, but we showed that when the MCF10As  
377 are grown in this physiologically appropriate two matrix system, they do not show an invasive phenotype  
378 with increased stromal stiffness.

379  
380 Similar to the methods described above to investigate the tumor microenvironment, studies of normal  
381 epithelial biology in 3D have also typically started from single cells seeded in a collagen-I matrix, and then  
382 allowed to develop for 10-12 days into mature cysts (Montesano 1991, reviewed in Zegers 2003, Belmonte  
383 2008). In other studies, cells were seeded in Matrigel® instead (Belmonte 2008). In both cases, the  
384 organization of the model did not fully recapitulate normal tissue arrangement. In addition, another  
385 drawback to this approach is that during the long incubation necessary to achieve fully polarized spheroids,

386 some cells can migrate away from the spheroid to the edge of the gel, where they form a 2D monolayer that  
387 can interfere with imaging, and perhaps alter the mechanical properties of the matrix.

388  
389 We have found that growing cells in a sub-gelation concentration of Matrigel® prior to seeding them in  
390 collagen-I promotes the formation of small multi-cell clusters (nucleated aggregates). Seeded into the  
391 collagen gel, these starter spheroids develop into mature spheroids in ~5-6 days, thus shortening the  
392 experiment preparation time by ~60% or up to 6 days. Alternatively, spheroids can be grown to full  
393 polarization in the dilute Matrigel® solution before incorporation into the collagen-I gel, which further  
394 increases the maturation speed, with most spheroids ready to use by day 4.

395  
396 Another major issue in 3D cell culture is that it is difficult to perform genetic manipulations on cells that  
397 are encapsulated in a hydrogel. One way around this limitation is to create stably transfected cell lines with  
398 a drug-inducible construct. Here we have developed methods to manipulate cells while they are growing in  
399 the dilute Matrigel® solution via methods such as electroporation (Nucleofection™), lipid-based reagents  
400 or iron-oxide nanoparticles (Magnetofection™). We have recently used this model system to investigate  
401 the mechanisms of epithelial morphogenesis and have shown that spheroids grown with this method display  
402 the same markers of polarity and respond to growth factor stimulation in the same way as the traditional  
403 spheroids grown in collagen-I (Bogorodskaya and Ligon, *submitted*).

#### 404 405 **Controls and caveats**

406 While we discuss the basics of spheroid formation and collagen-I hydrogels, it is important to note that  
407 there are a large number of parameters that can affect the properties of the model system. Altering a  
408 parameter can drastically change the collagen-I fiber size, hydrogel porosity, mechanical properties,  
409 spheroid size, spheroid number and cell survival.

410  
411 As with any culture system, selection of cell culture media is critical and the effects of different media on  
412 all cell types used in the system must be evaluated. Cross-linkers can cause viability issues with some cell  
413 types, so we also recommend evaluating the viability of your cells after incorporation into the PEG-diNHS  
414 cross-linked collagen-I stromal hydrogel. Finally, there are many opportunities for variation in preparing  
415 the various reagents used in making the hydrogels, so we also recommend evaluating the stiffness of the  
416 collagen-I hydrogels to ensure that they are of desired stiffness. We have done so via bulk rheometry, but  
417 other methods such as extensiometry (Drury et al., 2004), nano-indentation by Atomic Force Microscopy  
418 (Soofi et al., 2009), or even embedded magnetic particles (Chippada et al., 2009) could be used as well.

#### 419 420 **Limitations**

421 The initial size of spheroids may be potentially limiting for some experimental scenarios. Although it is  
422 possible to generate very large spheroids, for this method, the spheroid must fit through the opening of  
423 micropipette tips (we use 200 µL tips for all of our spheroid handling) and scale to the volume of the tip.  
424 This limitation is however easily overcome by using larger pipettes and larger volumes of hydrogel.  
425 Although we have observed no nutrient limitation or waste product induced cell death at the scale we have  
426 used (spheroids up to ~2 mm<sup>3</sup>), these are potential concerns for larger spheroids. For polarized cysts, the  
427 size of the resulting cyst will be dependent on the initial starter spheroid, and high variability of cyst sizes  
428 is possible, with spheroids ranging from 100 µm to 500 µm and larger in diameter. For cysts left to mature

429 in Matrigel® suspension, most of the cysts will be ready on day 4, but those left in Matrigel® will continue  
430 increasing in size, reaching up to 500 µm in diameter.

431

432

### 433 ACKNOWLEDGEMENTS

434

435 We would like to thank Mariah Hahn and Ryan Gilbert as well as members of their labs, and former Ligon  
436 lab member Joseph Wiegartner for their assistance with biomaterials. This work has been supported by the  
437 American Cancer Society Research Scholar Grant (RSG-10-245-01-CSM) and by the National Institutes  
438 of Health grant R01GM098619.

439

### 440 REFERENCES

441

- 442 Abdella, P.M., P.K. Smith, and G.P. Royer. 1979. A new cleavable reagent for cross-linking and  
443 reversible immobilization of proteins. *Biochem. Biophys. Res. Commun.* 87:734–42.
- 444 Azab, A.K., B. Orkin, V. Doviner, A. Nissan, M. Klein, M. Srebnik, and A. Rubinstein. 2006.  
445 Crosslinked chitosan implants as potential degradable devices for brachytherapy: In vitro and in  
446 vivo analysis. *J. Control. Release.* 111:281–289. doi:10.1016/j.jconrel.2005.12.014.
- 447 Barralet, J.E., L. Wang, M. Lawson, J.T. Triffitt, P.R. Cooper, and R.M. Shelton. 2005. Comparison of  
448 bone marrow cell growth on 2D and 3D alginate hydrogels. *J. Mater. Sci. Mater. Med.* 16:515–519.  
449 doi:10.1007/s10856-005-0526-z.
- 450 Batorsky, A., J. Liao, A.W. Lund, G.E. Plopper, and J.P. Stegemann. 2005. Encapsulation of adult human  
451 mesenchymal stem cells within collagen-agarose microenvironments. *Biotechnol. Bioeng.* 92:492–  
452 500. doi:10.1002/bit.20614.
- 453 Bischel, L.L., D.J. Beebe, and K.E. Sung. 2015. Microfluidic model of ductal carcinoma in situ with 3D,  
454 organotypic structure. *BMC Cancer.* 15:1–10. doi:10.1186/s12885-015-1007-5.
- 455 Chambers, K.F., J.F. Pearson, N. Aziz, P. O’Toole, D. Garrod, and S.H. Lang. 2011. Stroma regulates  
456 increased epithelial lateral cell adhesion in 3D culture: a role for actin/cadherin dynamics. *PLoS*  
457 *One.* 6:e18796. doi:10.1371/journal.pone.0018796.
- 458 Chenite, A., M. Buschmann, D. Wang, C. Chaput, and N. Kandani. 2001. Rheological characterisation of  
459 thermogelling chitosan/glycerol-phosphate solutions. *Carbohydr. Polym.* 46:39–47.  
460 doi:10.1016/S0144-8617(00)00281-2.
- 461 Chia, H.N., M. Vigen, and a. M. Kasko. 2012. Effect of substrate stiffness on pulmonary fibroblast  
462 activation by TGF-β. *Acta Biomater.* 8:2602–2611. doi:10.1016/j.actbio.2012.03.027.
- 463 Chippada, U., B. Yurke, P.C. Georges, and N. a. Langrana. 2009. A noninvasive method of measuring  
464 the local mechanical properties of soft hydrogels using magnetic microneedles. *J. Biomech. Eng.*  
465 131:21014. doi:10.1115/1.3005166.
- 466 Culav, E.M., C.H. Clark, and M.J. Merrilees. 1999. Connective tissues: matrix composition and its  
467 relevance to physical therapy. *Phys. Ther.* 79:308–319.
- 468 Deng, C., P. Zhang, B. Vulesevic, D. Kuraitis, F. Li, A.F. Yang, M. Griffith, M. Ruel, and E.J. Suuronen.  
469 2010. A collagen–chitosan hydrogel for endothelial differentiation and angiogenesis. *Tissue Eng.*  
470 *Part A.* 16:3099–109. doi:10.1089/ten.tea.2009.0504.
- 471 Drury, J.L., R.G. Dennis, and D.J. Mooney. 2004. The tensile properties of alginate hydrogels.  
472 *Biomaterials.* 25:3187–3199. doi:10.1016/j.biomaterials.2003.10.002.
- 473 Gandavarapu, N.R., M.A. Azagarsamy, and K.S. Anseth. 2014. Photo-click living strategy for controlled,  
474 reversible exchange of biochemical ligands. *Adv. Mater.* 26:2521–2526.  
475 doi:10.1002/adma.201304847.
- 476 Hughes, C.S., L.M. Postovit, and G. a. Lajoie. 2010. Matrigel: a complex protein mixture required for  
477 optimal growth of cell culture. *Proteomics.* 10:1886–1890. doi:10.1002/pmic.200900758.

- 478 Jeong, J.H., Y. Liang, M. Jang, C. Cha, C. Chu, H. Lee, W. Jung, J.W. Kim, S.A. Boppart, and H. Kong.  
479 2013. Stiffness-modulated water retention and neovascularization of dermal fibroblast-encapsulating  
480 collagen gel. *Tissue Eng. Part A*. 19:1275–1284. doi:10.1089/ten.TEA.2012.0230.
- 481 Kalluri, R. 2003. Basement membranes: structure, assembly and role in tumour angiogenesis. *Nat. Rev.*  
482 *Cancer*. 3:422–433. doi:10.1038/nrc1094.
- 483 Kimlin, L.C., G. Casagrande, and V.M. Virador. 2013. In vitro three-dimensional (3D) models in cancer  
484 research: An update. *Mol. Carcinog.* 52:167–182. doi:10.1002/mc.21844.
- 485 Krause, S., M. V Maffini, A.M. Soto, and C. Sonnenschein. 2008. A novel 3D in vitro culture model to  
486 study stromal-epithelial interactions in the mammary gland. *Tissue Eng. Part C. Methods*. 14:261–  
487 271. doi:10.1089/ten.tec.2008.0030.
- 488 Leight, J.L., M. a Wozniak, S. Chen, M.L. Lynch, and C.S. Chen. 2012. Matrix rigidity regulates a switch  
489 between TGF- $\beta$ 1-induced apoptosis and epithelial-mesenchymal transition. *Mol. Biol. Cell*. 23:781–  
490 791. doi:10.1091/mbc.E11-06-0537.
- 491 Levental, K.R., H. Yu, L. Kass, J.N. Lakins, M. Egeblad, J.T. Erler, S.F.T. Fong, K. Csiszar, A. Giaccia,  
492 W. Weninger, M. Yamauchi, D.L. Gasser, and V.M. Weaver. 2009. Matrix crosslinking forces  
493 tumor progression by enhancing integrin signaling. *Cell*. 139:891–906.  
494 doi:10.1016/j.cell.2009.10.027.
- 495 Li, X., X. Ma, D. Fan, and C. Zhu. 2012. New suitable for tissue reconstruction injectable  
496 chitosan/collagen-based hydrogels. *Soft Matter*. 8:3781–3790. doi:10.1039/c2sm06994f.
- 497 Li, Y., A. Asadi, M.R. Monroe, and E.P. Douglas. 2009. pH effects on collagen fibrillogenesis in vitro:  
498 Electrostatic interactions and phosphate binding. *Mater. Sci. Eng. C*. 29:1643–1649.  
499 doi:10.1016/j.msec.2009.01.001.
- 500 Liang, Y., J. Jeong, R.J. DeVolder, C. Cha, F. Wang, Y.W. Tong, and H. Kong. 2011. A cell-instructive  
501 hydrogel to regulate malignancy of 3D tumor spheroids with matrix rigidity. *Biomaterials*. 32:9308–  
502 9315. doi:10.1016/j.biomaterials.2011.08.045.
- 503 Liu, S.Q., Q. Tian, J.L. Hedrick, J.H. Po Hui, P.L. Rachel Ee, and Y.Y. Yang. 2010. Biomimetic  
504 hydrogels for chondrogenic differentiation of human mesenchymal stem cells to neocartilage.  
505 *Biomaterials*. 31:7298–7307. doi:10.1016/j.biomaterials.2010.06.001.
- 506 Martens, P. 2000. Characterization of hydrogels formed from acrylate modified poly(vinyl alcohol)  
507 macromers. *Polymer (Guildf)*. 41:7715–7722. doi:10.1016/S0032-3861(00)00123-3.
- 508 Masters, K.S., D.N. Shah, G. Walker, L. a. Leinwand, and K.S. Anseth. 2004. Designing scaffolds for  
509 valvular interstitial cells: Cell adhesion and function on naturally derived materials. *J. Biomed.*  
510 *Mater. Res. - Part A*. 71:172–180. doi:10.1002/jbm.a.30149.
- 511 McKay, C.A., R.D. Pomrenke, J.S. McLane, N.J. Schaub, E.K. Desimone, L.A. Ligon, and R.J. Gilbert.  
512 2014. An injectable, calcium responsive composite hydrogel for the treatment of acute spinal cord  
513 injury. *ACS Appl. Mater. Interfaces*. 6:1424–1438. doi:10.1021/am4027423.
- 514 McLane, J.S., and L.A. Ligon. 2015. Palladin mediates stiffness induced fibroblast activation in the tumor  
515 microenvironment. *Biophys. J*. 109:249–264. doi:10.1016/j.bpj.2015.06.033.
- 516 McLane, J.S., and L.A. Ligon. 2016. Stiffened extracellular matrix and signaling from stromal fibroblasts  
517 via osteoprotegerin combine to result in regulation of tumor cell invasiveness in a 3-D model of a  
518 tumor in situ. *Cancer Microenviron*. 9:127–139. doi:10.1007/s12307-016-0188-z.
- 519 McLane, J.S., C.J. Rivet, R.J. Gilbert, and L.A. Ligon. 2014a. A biomaterial model of tumor stromal  
520 microenvironment promotes mesenchymal morphology but not epithelial to mesenchymal transition  
521 in epithelial cells. *Acta Biomater*. 10:4811–4821. doi:10.1016/j.actbio.2014.07.016.
- 522 McLane, J.S., C.J. Rivet, R.J. Gilbert, and L.A. Ligon. 2014b. A biomaterial model of tumor stromal  
523 microenvironment promotes mesenchymal morphology but not epithelial to mesenchymal transition  
524 in epithelial cells. *Acta Biomater*. 10:4811–21. doi:10.1016/j.actbio.2014.07.016.
- 525 Munoz-Pinto, D.J., A.C. Jimenez-Vergara, Y. Hou, H.N. Hayenga, A. Rivas, M. Grunlan, and M.S. Hahn.  
526 2012. Osteogenic potential of poly(ethylene glycol)–poly(dimethylsiloxane) hybrid hydrogels.  
527 *Tissue Eng. Part A*. 18:1710–1719. doi:10.1089/ten.tea.2011.0348.
- 528 Paszek, M.J., N. Zahir, K.R. Johnson, J.N. Lakins, G.I. Rozenberg, A. Gefen, C. a Reinhart-King, S.S.

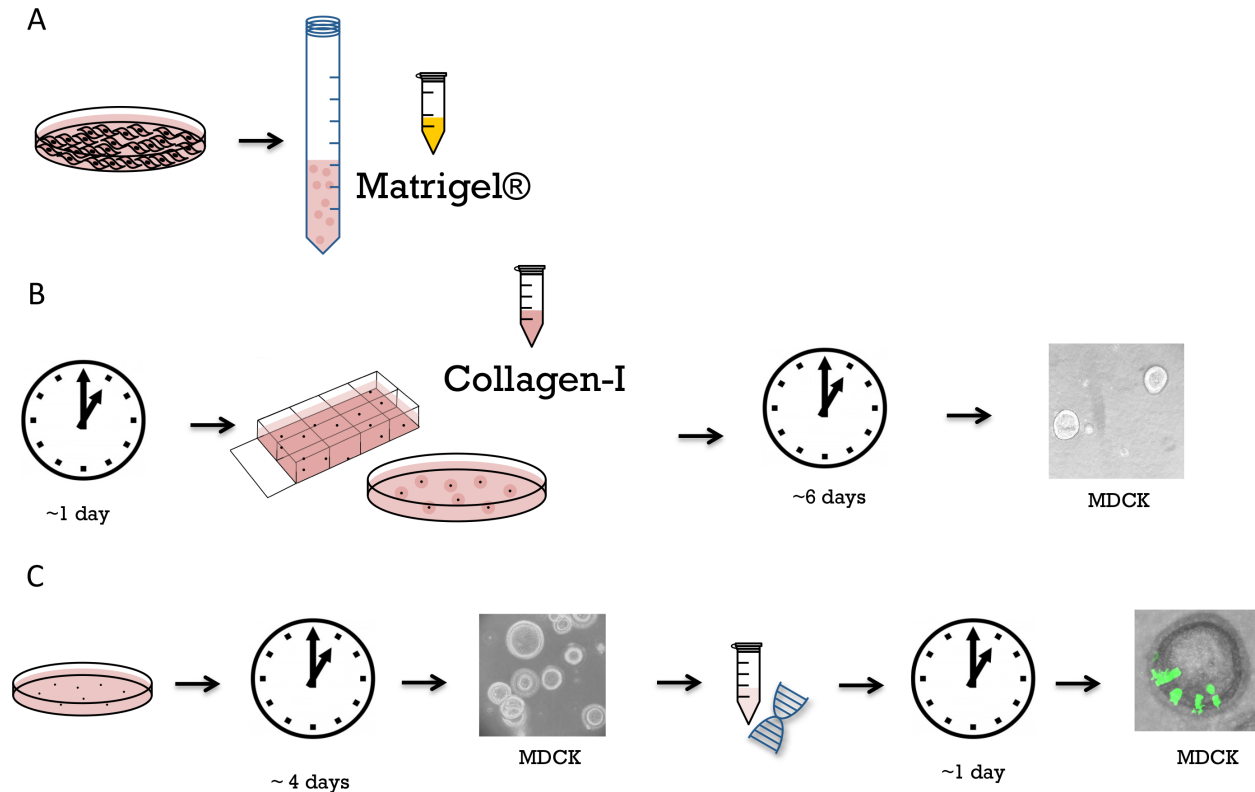


- 529 Margulies, M. Dembo, D. Boettiger, D. a Hammer, and V.M. Weaver. 2005. Tensional homeostasis  
530 and the malignant phenotype. *Cancer Cell*. 8:241–254. doi:10.1016/j.ccr.2005.08.010.
- 531 Pathak, A., and S. Kumar. 2012. Independent regulation of tumor cell migration by matrix stiffness and  
532 confinement. *Proc. Natl. Acad. Sci. U. S. A.* 109:10334–9. doi:10.1073/pnas.1118073109.
- 533 Peng, Q., L. Zhao, Y. Hou, Y. Sun, L. Wang, H. Luo, H. Peng, and M. Liu. 2013. Biological  
534 characteristics and genetic heterogeneity between carcinoma-associated fibroblasts and their paired  
535 normal fibroblasts in human breast cancer. *PLoS One*. 8:e60321. doi:10.1371/journal.pone.0060321.
- 536 Plant, A.L., K. Bhadriraju, T. a. Spurlin, and J.T. Elliott. 2009. Cell response to matrix mechanics: Focus  
537 on collagen. *Biochim. Biophys. Acta - Mol. Cell Res.* 1793:893–902.  
538 doi:10.1016/j.bbamcr.2008.10.012.
- 539 Richards, J., L. Larson, J. Yang, R. Guzman, Y. Tomooka, R. Osborn, W. Imagawa, and S. Nandi. 1983.  
540 Method for culturing mammary epithelial cells in a rat tail collagen gel matrix. *J. Tissue Cult.*  
541 *Methods*. 8:31–36. doi:10.1007/BF01834632.
- 542 Roeder, B.A., K. Kokini, J.E. Sturgis, J.P. Robinson, and S.L. Voytik-Harbin. 2002. Tensile Mechanical  
543 Properties of Three-Dimensional Type I Collagen Extracellular Matrices With Varied  
544 Microstructure. *J. Biomech. Eng.* 124:214. doi:10.1115/1.1449904.
- 545 Sawhney, A., C. Pathak, and J. Hubbell. 1993. Bioerodible hydrogels based on photopolymerized poly  
546 (ethylene glycol)-co-poly (alpha-hydroxy acid) diacrylate macromers. *Macromolecules*. 26:581–  
547 587. doi:10.1021/ma00056a005.
- 548 Shoulders, M.D., and R.T. Raines. 2009. Collagen structure and stability. *Annu. Rev. Biochem.* 78:929–  
549 958. doi:10.1146/annurev.biochem.77.032207.120833.
- 550 Song, K., M. Qiao, T. Liu, B. Jiang, H.M. Macedo, X. Ma, and Z. Cui. 2010. Preparation, fabrication and  
551 biocompatibility of novel injectable temperature-sensitive chitosan/glycerophosphate/collagen  
552 hydrogels. *J. Mater. Sci. Mater. Med.* 21:2835–42. doi:10.1007/s10856-010-4131-4.
- 553 Soofi, S.S., J.A. Last, S.J. Liliensiek, P.F. Nealey, and C.J. Murphy. 2009. The elastic modulus of  
554 Matrigel as determined by atomic force microscopy. *J. Struct. Biol.* 167:216–9.  
555 doi:10.1016/j.jsb.2009.05.005.
- 556 Swamydas, M., J.M. Eddy, K.J.L. Burg, and D. Dréau. 2010. Matrix compositions and the development  
557 of breast acini and ducts in 3D cultures. *Vitr. Cell. Dev. Biol. - Anim.* 46:673–684.  
558 doi:10.1007/s11626-010-9323-1.
- 559 Tilghman, R.W., C.R. Cowan, J.D. Mih, Y. Koryakina, D. Gioeli, J.K. Slack-Davis, B.R. Blackman, D.J.  
560 Tschumperlin, and J.T. Parsons. 2010. Matrix rigidity regulates cancer cell growth and cellular  
561 phenotype. *PLoS One*. 5:1–13. doi:10.1371/journal.pone.0012905.
- 562 Ulrich, T. a, A. Jain, K. Tanner, J.L. MacKay, and S. Kumar. 2010. Probing cellular mechanobiology in  
563 three-dimensional culture with collagen-agarose matrices. *Biomaterials*. 31:1875–84.  
564 doi:10.1016/j.biomaterials.2009.10.047.
- 565 Ulrich, T. a, T.G. Lee, H.K. Shon, D.W. Moon, and S. Kumar. 2011. Microscale mechanisms of agarose-  
566 induced disruption of collagen remodeling. *Biomaterials*. 32:5633–42.  
567 doi:10.1016/j.biomaterials.2011.04.045.
- 568 Viney, M.E., A.J. Bullock, M.J. Day, and S. MacNeil. 2009. Co-culture of intestinal epithelial and  
569 stromal cells in 3D collagen-based environments. *Regen. Med.* 4:397–406. doi:10.2217/rme.09.4.
- 570 Wallace, D. 2003. Collagen gel systems for sustained delivery and tissue engineering. *Adv. Drug Deliv.*  
571 *Rev.* 55:1631–1649. doi:10.1016/j.addr.2003.08.004.
- 572 Wang, H.B., M.E. Mullins, J.M. Cregg, A. Hurtado, M. Oudega, M.T. Trombley, and R.J. Gilbert. 2009.  
573 Creation of highly aligned electrospun poly-L-lactic acid fibers for nerve regeneration applications.  
574 *J. Neural Eng.* 6:16001. doi:10.1088/1741-2560/6/1/016001.
- 575 Wang, H.B., M.E. Mullins, J.M. Cregg, C.W. McCarthy, and R.J. Gilbert. 2010. Varying the diameter of  
576 aligned electrospun fibers alters neurite outgrowth and Schwann cell migration. *Acta Biomater.*  
577 6:2970–2978. doi:10.1016/j.actbio.2010.02.020.
- 578 Wang, L., and J.P. Stegmann. 2010. Thermogelling chitosan and collagen composite hydrogels initiated  
579 with beta-glycerophosphate for bone tissue engineering. *Biomaterials*. 31:3976–85.



580           doi:10.1016/j.biomaterials.2010.01.131.  
581       Wang, L., and J.P. Stegeman. 2011. Glyoxal crosslinking of cell-seeded chitosan/collagen hydrogels for  
582       bone regeneration. *Acta Biomater.* 7:2410–7. doi:10.1016/j.actbio.2011.02.029.  
583       Yang, Y.-L., L.M. Leone, and L.J. Kaufman. 2009. Elastic moduli of collagen gels can be predicted from  
584       two-dimensional confocal microscopy. *Biophys. J.* 97:2051–2060. doi:10.1016/j.bpj.2009.07.035.  
585       Yoshida, S., E. Shimizu, T. Ogura, M. Takada, and S. Sone. 1997. Stimulatory effect of reconstituted  
586       basement membrane components (matrigel) on the colony formation of a panel of human lung  
587       cancer cell lines in soft agar. *J. Cancer Res. Clin. Oncol.* 123:301–309.  
588       doi:10.1007/s004320050062.  
589  
590  
591  
592  
593  
594  
595

596



597

598

599

### Figure 1 Preparation of polarized epithelial spheroid model

600

601

602

603

604

605

606

607

608

609

A. Overnight incubation of the cells with dilute Matrigel®. Cells are trypsinized, counted and incubated with the sub-gelation concentration of Matrigel® (1 mg / mL) overnight in a 15 mL conical tube. The incubation results in formation of cell clumps, which are later used as starter material for polarized epithelial spheroids. B. Incorporation of epithelial spheroids into hydrogels immediately after overnight incubation. Cell clumps are incorporated into collagen-I gels using either a sandwich system in a 8-chamber slide or 100  $\mu$ L gel drops placed on the bottom of a 10 cm culture dish. Over the course of six days the spheroids grow and polarize. C. Growth of polarized epithelial spheroids in suspension. After overnight incubation with sub-gelation concentration of Matrigel® the cell clumps are transferred into a cell culture dish filled with culture media, in which they grow and polarize over the course of 4 days. The spheroids then can be transfected (optional) and seeded into hydrogel.

610

611

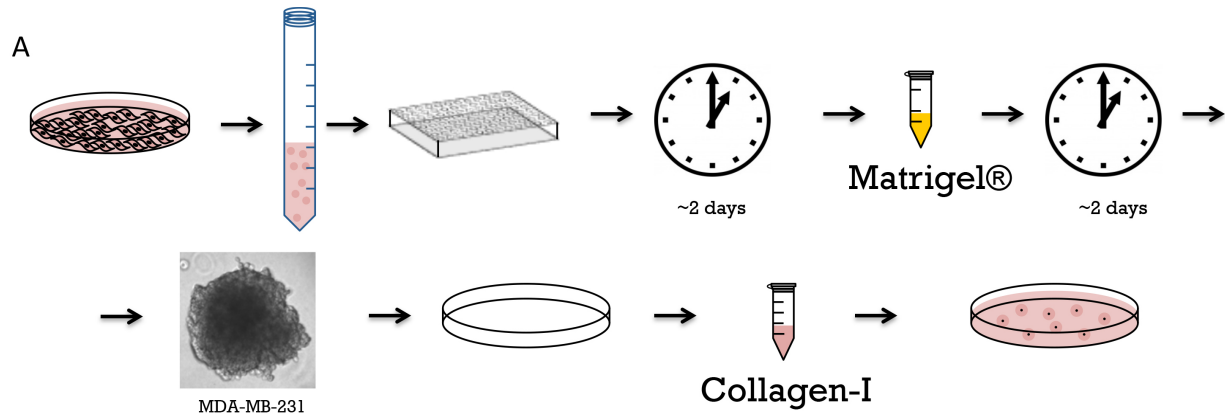


**Figure 2 Preparation of tumor spheroid model**

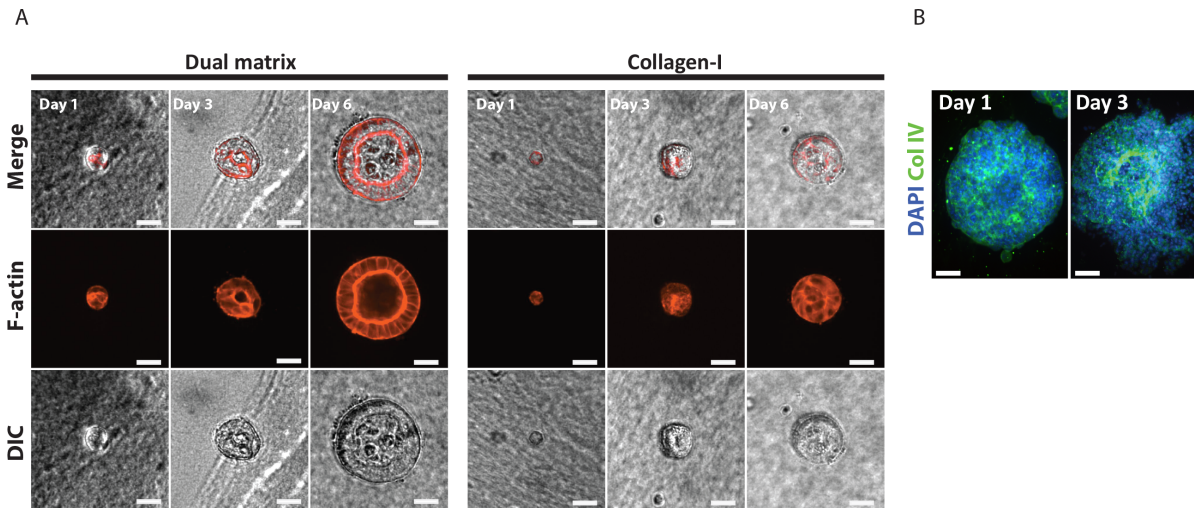
612 A. Tumor model preparation and seeding to collagen gel. Cells are trypsinized, counted and distributed  
613 into low-attachments 96-well plate, then incubated for two days, at which point cells coalesce. Sub-  
614 gelation concentration of Matrigel® (1 mg / mL) is then added to coalesced cells to provide basement  
615 membrane components and facilitate spheroid formation on the course of additional 48 hours. Formed  
616 spheroids are then incorporated into collagen gels and hydrogel droplets are placed in 10 cm cell culture  
617 dishes for further growth.

618  
619

620

621

622



623

624 **Figure 3 Polarized and tumor spheroids formation timeline.**

625 A. Comparison of speed of polarization of epithelial cells in dual-matrix versus collagen-I only culture.

626 Spheroids are grown either using dual matrix system (left panel), or only in collagen-I (right panel).

627 Spheroids are fixed on day 1, day 3 and day 6 in both systems and morphologies of spheroids are

628 compared through immunostaining for filamentous actin (phalloidin, red). Examples of spheroids in both

629 systems are shown for each day. Scale = 30  $\mu$ m. B. Tumor spheroids of MDA-MB231 breast cancer cells

630 grown in dual matrix system.

631

632